# Supplementary material for "PMP-Net: Point Cloud Completion by Learning Multi-step Point Moving Paths"

Xin Wen[1], Peng Xiang[1], Zhizhong Han[2], Yan-Pei Cao[3], Pengfei Wan[3], Wen Zheng[3], Yu-Shen Liu[1]*

[1]School of Software, BNRist, Tsinghua University, Beijing, China
[2]Department of Computer Science, Wayne State University, USA
[3] Y-tech, Kuaishou Technology, Beijing, China

{x-wen16,xp20}@mails.tsinghua.edu.cn  h312h@wayne.edu  caoyanpei@gmail.com

{wanpengfei,zhengwen}@kuaishou.com  liuyushen@tsinghua.edu.cn

## 1. Detailed Settings

We use the single scale grouping (SSG) version of Point-Net++ and its feature propagation module as the basic framework of PMP-Net. The detailed architecture of each part is described in Table 1 and Table 2, respectively.

Table 1. The detailed structure of encoder.

| Level | #Points | Radius | #Sample | MLPs |
|---|---|---|---|---|
| 1 | 512 | 0.2 | 32 | [64, 64, 128] |
| 2 | 128 | 0.4 | 32 | [128, 128, 256] |
| 3 | - | - | - | [256, 512, 1024] |

In Table 1, "#Points" denotes the number of down-sampled points, "Radius" denotes the radius of ball query, "#Sample" denotes the number of neighbors points sampled for each center point, "MLPs" denotes the number of output channels for MLPs in each level of encoder.

Table 2. The detailed architecture of feature propagation module.

| Level | 1 | 2 | 3 |
|---|---|---|---|
| MLPs | [256, 256] | [256, 128] | [128, 128, 128] |

**Training details.** We use AdamOptimizer to train PMP-Net with an initial learning rate $10^{-3}$, and exponentially decay it by 0.5 for every 20 epochs. The training process is accomplished using a single NVDIA GTX 2080TI GPU with a batch size of 24. PMP-Net takes 150 epochs to converge on both PCN and Completion3D dataset. We scale all input training shapes of Completion3D by 0.9 to avoid points out of the range of *tanh* activation.

## 2. More Experiments

### 2.1. Dimension of Noise Vector.

The noise vector in Eq.(1) in our paper is used to push the points to leave their original place. In this section, we analyze the dimension and the standard deviation of the noise, which may potentially decide the influence of the noise to the points. Because either the dimension or the standard deviation of the noise vector decreases to 0, there will be no disturbance in the network. On the other hand, larger vector dimension or standard deviation will cause larger disturbance in the network. In Table 3, we first analyze the influence of dimension of noise vector. By comparing 0-dimension result with others, we can draw conclusion that the disturbance caused by noise vector is important to learn the point deformation. And by analyzing the performance of different length of noise vector, we can find that the influence of vector length is relatively small, compared with the existence of noise vector.

Table 3. The effect of noise dimension (baseline marked by "*").

| Dim. | avg. | plane | chair | car | table |
|---|---|---|---|---|---|
| 0 | 14.56 | 4.39 | 10.48 | 19.01 | 24.33 |
| 8 | 11.85 | 3.28 | 7.95 | 15.65 | 20.50 |
| 16 | 11.68 | 3.44 | **7.86** | **15.22** | 20.19 |
| 32* | **11.58** | 3.42 | 7.87 | 15.88 | **19.15** |
| 64 | **11.58** | **3.14** | 7.96 | 16.01 | 19.17 |

### 2.2. Standard Deviation of Noise Distribution.

In Table 4, we show the completion results of PMP-Net under different standard deviations of noise vector. Similar to the analysis of vector dimension, we can draw conclusion that larger disturbance caused by bigger standard deviation will help the network achieve better completion performance. The influence of noise vector becomes weak when the standard deviation reaches certain threshold (around
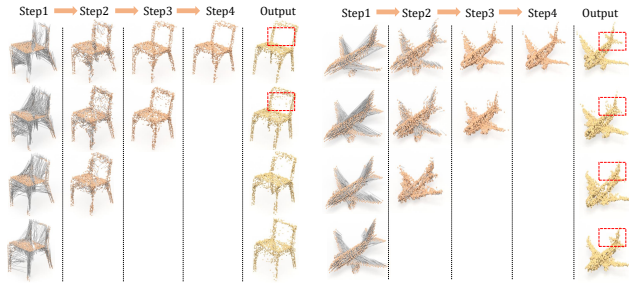
Figure 1. Illustration of multi-step searching under different searching steps. The first row is 4-step completion, and the second row is 3-step completion, and so on.

$10^{-1}$ according to Table 4).

Table 4. The effect of standard deviation (baseline marked by "*").

| Stddev. | Avg. | Plane | Chair | Car | Table |
|---------|------|-------|-------|-----|-------|
| $10^{-2}$ | 11.89 | 3.32 | 8.15 | 16.42 | 19.58 |
| $10^{-1}$ | **11.56** | 3.58 | 7.78 | 15.47 | 19.41 |
| 1.0* | 11.58 | 3.42 | **7.87** | 15.88 | **19.15** |
| 10 | 11.62 | **3.35** | 7.88 | **15.29** | 19.95 |

## 2.3. Visual Analysis of Multi-step Searching.

We visualize the point deformation process under different searching step sittings in Figure 1. Comparing the 4-step searching in the top-row with the other three sittings, the empty space on the chair back is shaped cleaner as highlighted by rectangles, which proves the effectiveness of multi-step searching to consistently refine the shape.

## 2.4. Visualization of Completion Results on PCN dataset.

In Figure 2 and Figure 3, we supplement results of shape completion on PCN dataset under each categories. For each category, the first row is the input incomplete shape, the second row is the predicted complete shape and the third row is the ground truth.
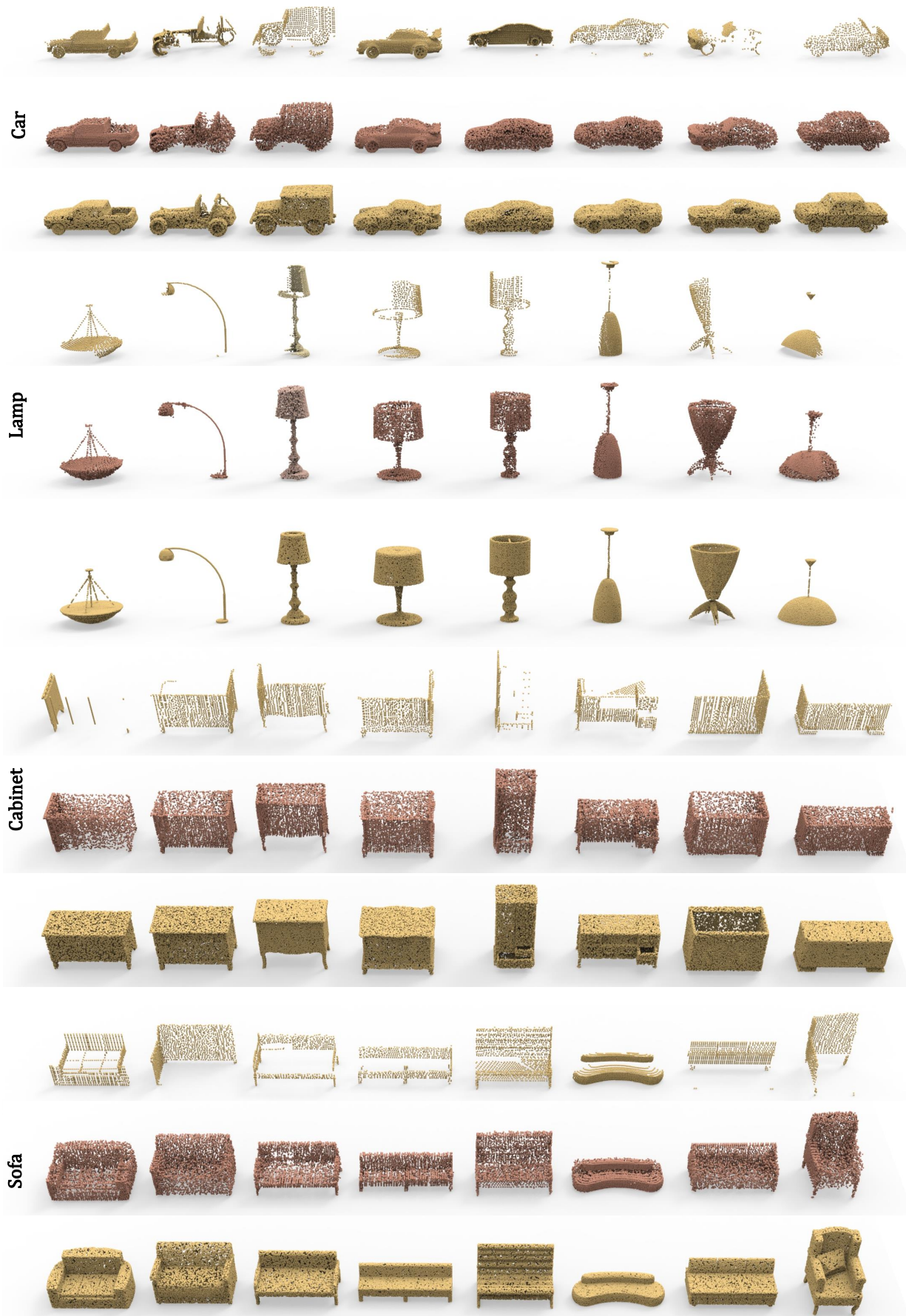
Figure 2. Illustration of shape completion on PCN dataset. For each category, the first row is the input incomplete shape, the second row is the predicted complete shape and the third row is the ground truth.

Figure 3. Illustration of shape completion on PCN dataset. For each category, the first row is the input incomplete shape, the second row is the predicted complete shape and the third row is the ground truth.